and (14)) are valid. Once T(s) and $\phi(s)$ are solved for, equation (23) relates the kite angle θ to the section lift/drag ratio, ℓ/d, in the form

$$\frac{d\theta}{ds} = \frac{\ell}{d}\frac{\sin\phi}{T} \tag{25}$$

Note that for $\ell/d \sim O(1)$, substantial kiting is possible, as would be expected from physical reasoning. At the same time, $\ell/d \sim O(1)$ implies very small angles of attack, viz.:

$$\alpha \sim \frac{\ell}{d}\frac{C_d}{\left(\frac{dC_\ell}{d\alpha}\right)_{\alpha = 0}} \sim (1)\ \frac{.02}{2\pi} \sim .003_{\text{RADIANS}} \tag{26}$$

In general $\alpha(s)$ must be solved from the twist moment equation (21). Under those circumstances when $\alpha(s)$ is a constant (these will be determined later) so is ℓ/d and equation (25) is easily integrated. Solutions for ϕ, T, and θ, corresponding to four selected drag loading functions, are summarized in Table 2. For simplicity, the boundary conditions at the body have been selected to be $\phi(o) = 90$ degrees (body drag/lift ratio is zero) and $\theta(o) = 0$ (body exerts no lateral force). The towing catenaries corresponding to the case $\alpha \equiv o$ are shown in Figure 4. The kite angle is shown as a function of scope in Figure 5.

This angle is weakly dependent on the particular form of loading function. Also, for reasonable scopes, the variation in kite from the extreme case of a vertical trail is small. For a scope $\frac{Sd}{T_o} = 1.0$, the lateral displacement as a function of cable lift-to-drag ratio is shown in Figure 6. The depth loss due to kiting is shown in Figure 7. This is normally less than 10 percent, even at kite angles up to 45 degrees. In summary, the effect of a small constant angle of attack is a substantial lateral body displacement, large kite angles in the upper part of the towline, and a small loss in depth. No change in trail occurs if the increase in drag due to angle of attack is neglected.

EFFECT OF CAMBER

Fairings are usually designed as symmetric hydrofoils sections. The presence of asymmetry (or camber) in the fairing cross section shape due, for example, to manufacturing limitations or deformation under use is recognized as a cause of kiting. If torsional and flexural stiffness effects on the towline twist are neglected, a simple physical interpretation of the mechanism of camber induced kiting and formulas for predicting the kiting can be derived.

Table 2 - Loading and Configuration Functions for Kiting Towline
With Constant Angle of Attack

ITEM		1	2	3	4
TANGENTIAL LOADING	σ_s/d	$\sin\phi\cos\phi$	0	$\cos\phi$	0
NORMAL LOADING	σ_n/d	$\sin^2\phi$	$\sin^2\phi$	$\sin\phi$	$\sin\phi$
TENSION	T/T_o	$\csc\phi$	1	$\csc\phi$	1
SCOPE	sd/T_o	$\frac{1}{2}(\ln[\cot\phi/2] + \cot\phi\csc\phi)$	$\cot\phi$	$\cot\phi$	$\ln[\cot\phi/2]$
TRAIL	xd/T_o	$\frac{1}{2}\cot^2\phi$	$\csc\phi - 1$	$\csc\phi - 1$	$\ln[\csc\phi]$
$\mathrm{DEPTH}\vert_{\alpha=0}$	Yd/T_o	$\cot\phi$	$\ln[\cot\phi/2]$	$\ln[\cot\phi/2]$	$\pi/2 - \phi$
KITE ANGLE	$\theta d/\ell$	$\ln[\tan\phi/2]$	$\ln[\tan\phi/2]$	$\phi - \pi/2$	$\phi - \pi/2$
DEPTH	Yd/T_o	$\frac{1}{1+\left(\frac{\ell}{d}\right)^2}\cot\phi\cos\theta - \frac{\ell/d}{1+\left(\frac{\ell}{d}\right)^2}\sin\theta\csc\phi$	$-(d/\ell)\sin\theta$	$\int_0^{\pi/2-\phi}\frac{\cos\left(\frac{\ell}{d}\right)r}{\cos r}\,dr$	$-\left(\frac{d}{\ell}\right)\sin\theta$
SIDE TRAIL	Zd/T_o	$\frac{1}{1+\left(\frac{\ell}{d}\right)^2}\cot\phi\sin\theta + \frac{\ell/d}{1+\left(\frac{\ell}{d}\right)^2}(\cos\theta\cos\phi - 1)$	$(d/\ell)(\cos\theta - 1)$	$-\int_0^{\pi/2-\phi}\frac{\sin\frac{\ell}{d}r}{\cos r}\,dr$	$(d/\ell)(\cos\theta - 1)$

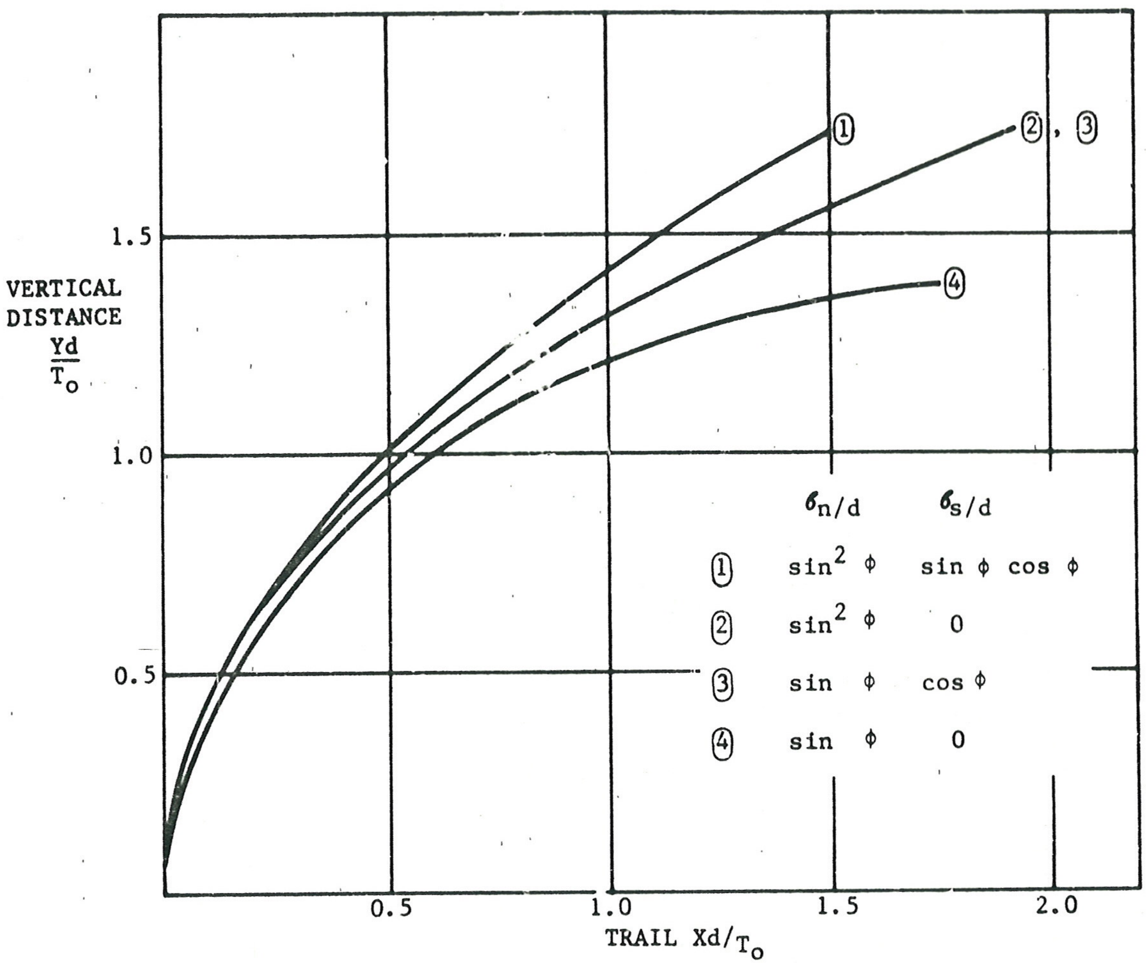

Figure 4 - Nondimensional Catenaries for Four Loading Functions

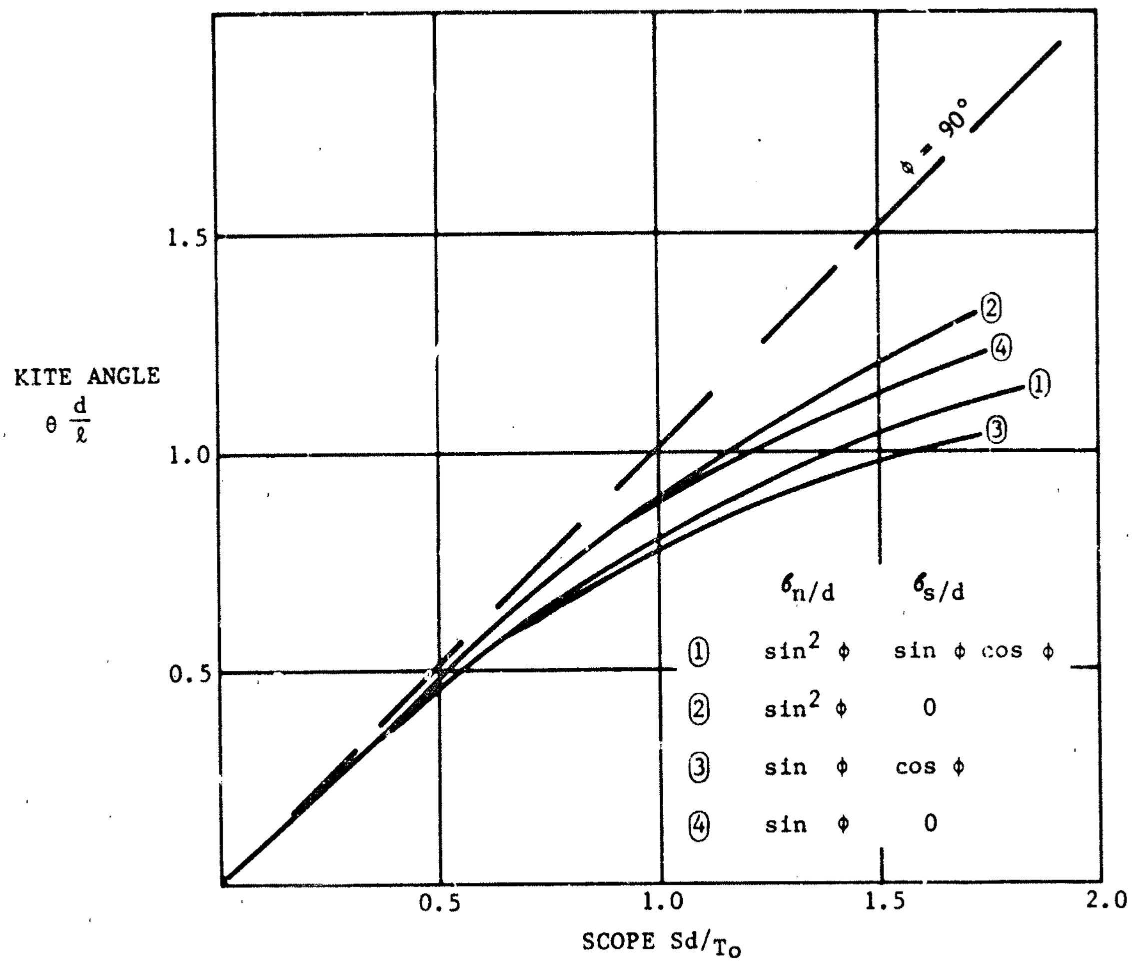

Figure 5 - Kite Angle as a Function of Scope

Consider the twist moments and kiting forces on a section of a cambered towline initially at zero angle of attack. The fairing will rotate until an equilibrium of moments is reached at some angle α_e, such that $m_s(\alpha_e) = 0$. (The moment in this case is referred to the effective center of tension.) In general, however, the kiting force $f_k(\alpha_e)$ is not zero. Thus, the towline will displace laterally until the tension force (TK_k) balances $f_k(\alpha_e)$ (equation (23)). This is shown schematically in Figure 8, where, for simplicity the lift due to camber ℓ_c, and angle of attack ℓ_α, are shown as separate, additive effects.

For moment equilibrium,

$$\ell_\alpha(\xi_\alpha - \xi_T) - \ell_c(\xi_c - \xi_T) = 0$$

or (27)

$$\ell_\alpha = \ell_c \frac{\xi_c - \xi_T}{\xi_\alpha - \xi_T}$$

where ξ_α, ξ_c, and ξ_T are the chordwise positions of the hydrodynamic and tension forces measured from the leading edge. The hydrodynamic kiting force, f_k, is

$$f_k = \ell_c - \ell_\alpha$$

(28)

$$= \ell_c \left(1 - \frac{\xi_c - \xi_T}{\xi_\alpha - \xi_T}\right)$$

In terms of the camber lift coefficient C_c defined as

$$C_c \equiv \ell_c/\rho/_2 V^2 C \tag{29}$$

the lift-to-drag ratio may be written as

$$\ell/d = f_k/d = C_c/C_d \left(1 - \frac{\xi_c - \xi_T}{\xi_\alpha - \xi_T}\right) \tag{30}$$

and the angle of attack α_e

$$\alpha_e = \frac{C_c}{\left(\frac{dC_\ell}{d\alpha}\right)_{\alpha = 0}} \cdot \frac{\xi_c - \xi_T}{\xi_\alpha - \xi_T} \tag{31}$$

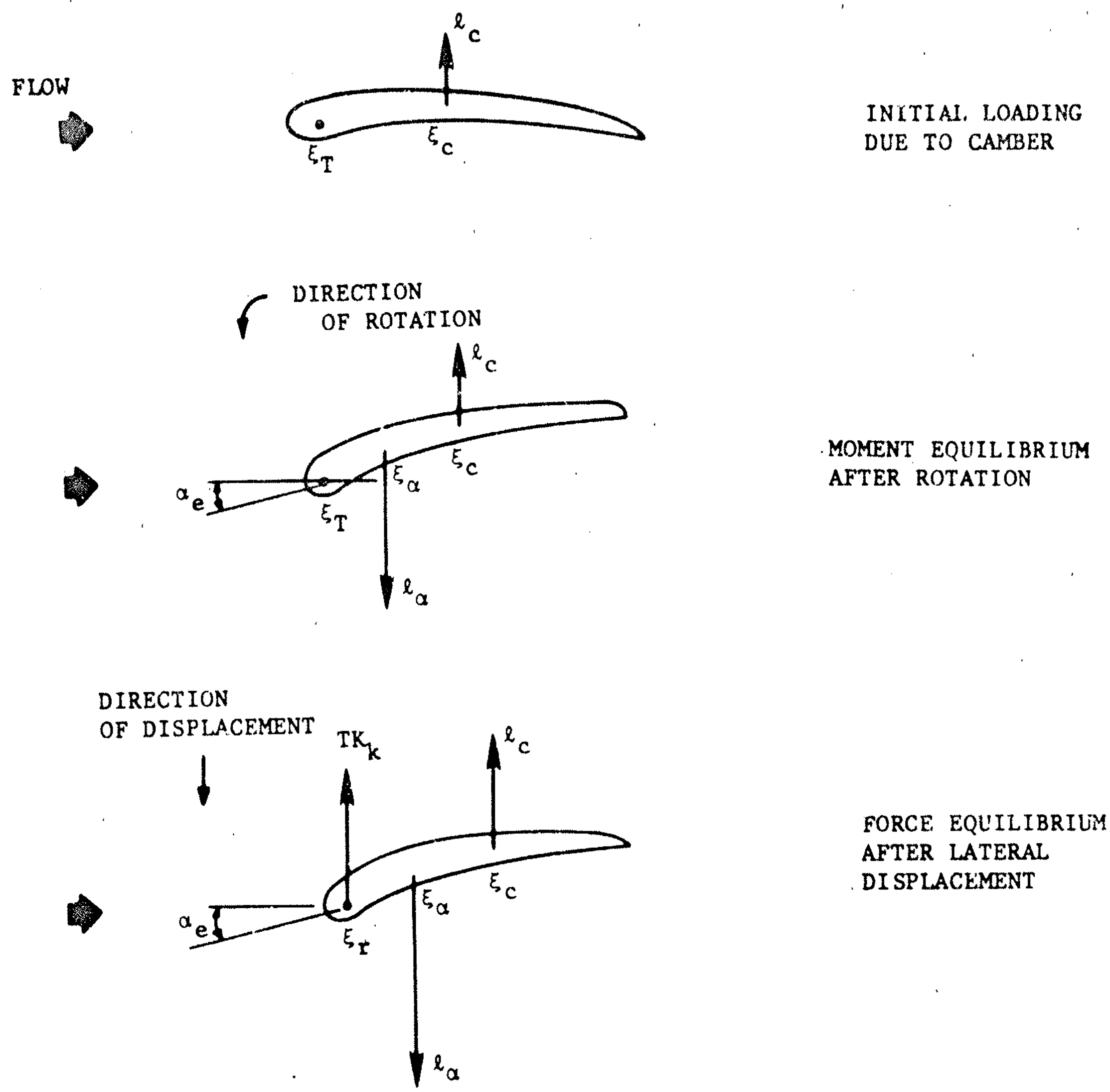

Figure 8 - Camber Induced Kiting

In the linear approximation, C_c is proportional to the camber/chord ratio, $\frac{C_o}{C}$. Thus, for a prescribed camber distribution and drag coefficient,

$$\frac{\ell}{d} \propto \left(\frac{C_o}{C}\right) \left(1 - \frac{\xi_c - \xi_T}{\xi_\alpha - \xi_T}\right) \tag{32}$$

This relationship is graphically presented in Figure 9 for a parabolic camber profile. Extermely small camber ratios, constant along the span, result in sufficient angles of attack and corresponding lift/drag ratios to cause significant kiting. The sensitivity to position of center of tension and center of pressure also is apparent. The center of pressure is primarily a function of the shape and construction of the fairing. The center of tension is located by the choice of shape, material and construction of the cable strength member.

It should be noted that a spanwise sinusiodal distribution of camber, with sufficiently small wavelength, will substantially reduce the degree of kiting. For example, a vertical cable ($\phi = 90°$) of length L with angle of attack $\alpha = \alpha_o \sin n\pi S/L$ (n = integer) has a lateral displacement Z(o), due to kiting of

$$\frac{Z(o)}{L} = \left(-\frac{dC_\ell}{d\alpha}\right)_{\alpha = 0} \cdot \frac{\rho/_2 V^2 CL}{T_o} \cdot \frac{\alpha_o}{n\pi} \tag{33}$$

EFFECT OF FLEXURAL RIGIDITY

In an integrated towline, the strength member is usually shaped such that bending in the towing catenary introduces destabilizing torsional moments. This is a consequence of the fairing streamlined shape and the desire to fill as much of the area as possible with tension carrying fibers. It is of interest to determine under what circumstances the towline is subject to torsional buckling instability. That is, the towline, if subjected to small disturbances, will assume divergent angles of attack and subsequent kiting.

If torsional rigidity effects are neglected ($\overline{GJ} \equiv 0$), the twist equation with s chosen as the elastic axis reduces to

$$-M_k K_k - M_n K_n + m_s \geq 0; \ \alpha > 0 \tag{34}$$

Since each cable section now acts independently in twist, the requirement for stability is a positive net moment for positive α (a restoring moment). Substituting the $\vec{M}$ components from Equation (17) and combining terms gives

$$T(\xi_T - \xi_s)(K_k - \alpha K_n) + (\overline{EI}_2 - \overline{EI}_1)(\alpha K_n^{\,2} - \alpha K_k^{\,2} - K_n K_k) + m_s \geq 0 \tag{35}$$

This can be written, using equations (19) and (20) as

$$T(\xi_T - \xi_s)K_n\left(\frac{f_k}{f_n} - \alpha\right) + (\overline{EI}_2 - \overline{EI}_1)(K_n^{\,2})\left[\alpha - \alpha\left(\frac{f_k}{f_n}\right)^2 - \frac{f_k}{f_n}\right] + m_s \geq 0 \tag{36}$$

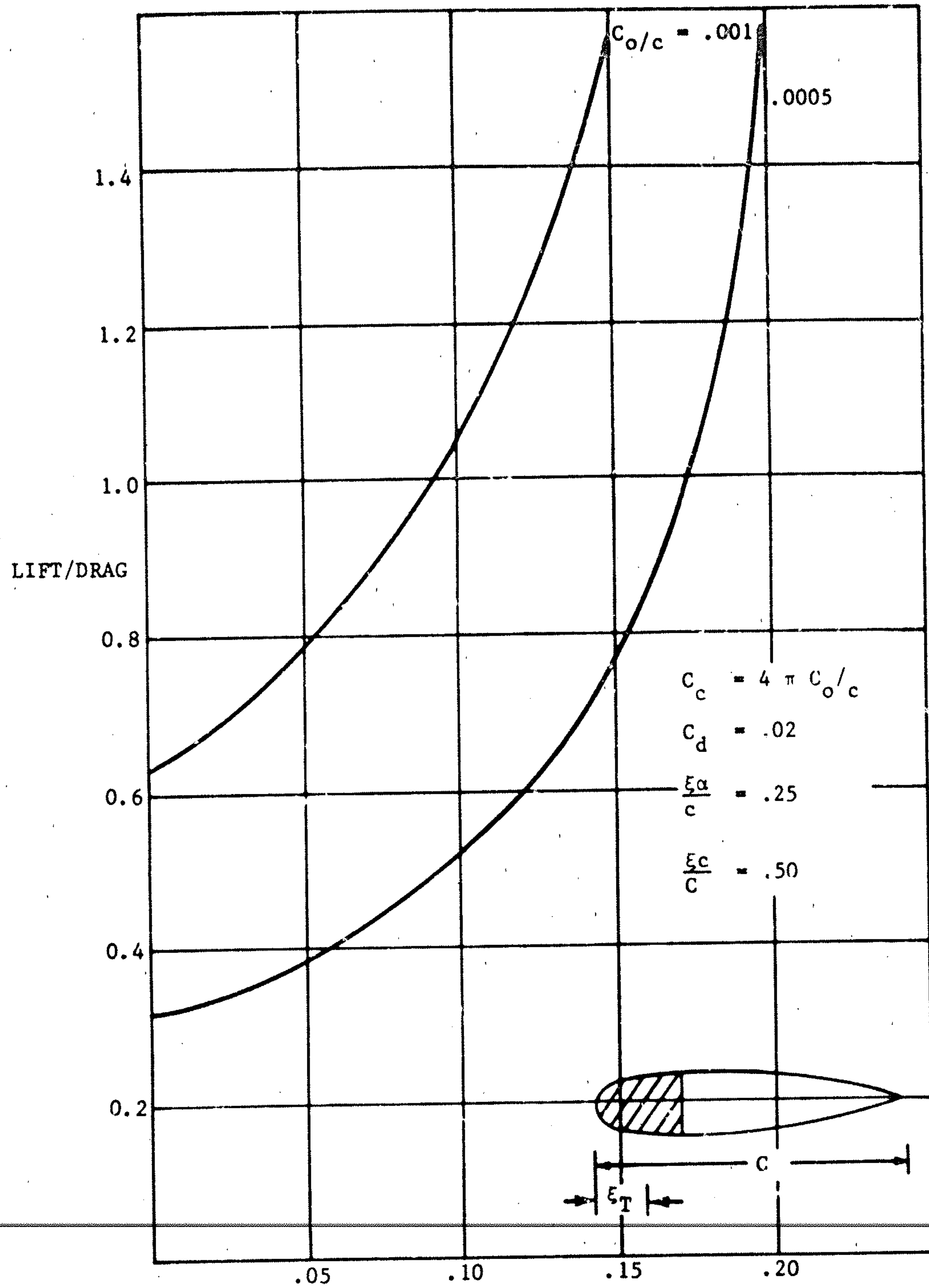

Figure 9 - Lift/Drag of a Kiting Faired Cable With Parabolic Camber

In the stability analysis, we are concerned with cases of $f_k/f_n < 1$ and since $\alpha << f_k/f_n$, equation (36) simplifies to

$$T(\xi_T - \xi_s) K_n \cdot \frac{f_k}{f_n} + (\overline{EI}_2 - \overline{EI}_1)(K_n^2)\left(-\frac{f_k}{f_n}\right) + m_s \geq 0 \tag{37}$$

or

$$-(\xi_T - \xi_s) + \frac{\overline{EI}_2 - \overline{EI}_1}{TR} + \frac{m_s}{f_k} \geq 0 \tag{38}$$

where R is the local radius of curvature in the ϕ plane $(-\frac{1}{K_n})$. Using equations (14) and (15), this may be written as

$$-(\xi_T - \xi_s) + \frac{\overline{EI}_2 - \overline{EI}_1}{TR} + \frac{m(\alpha)}{\ell(\alpha)} \geq 0 \tag{39}$$

If the approximation

$$m(\alpha) \approx \ell(\alpha) \cdot (\xi_\alpha - \varepsilon_s) \tag{40}$$

is used, where ξ_α is the chordwise position of the center of lift, then the requirement for twist stability becomes

$$\xi_\alpha - \xi_T \geq \frac{\overline{EI}_1 - \overline{EI}_2}{TR} \tag{41}$$

Since the structural destabilizing moment and the hydrodynamic restoring moment are both nearly linearly dependent on lift coefficient, it does not appear in equation (41). The speed of tow enters only implicity in determining the tension and radius of curvature. It may be concluded from equation (41) that flexural stiffness acts to reduce the effective hydrodynamic restoring moment arm $(\xi_\alpha - \xi_T)$. As an example of application of equation (41), consider the integrated towline developed by the Boeing Company in conjunction with the Naval Undersea Center.[9] The characteristics are:

$\overline{EI}_1$	= 25,420 lb in^2	
$\overline{EI}_2$	= 17,340 lb in^2	
T	= 10,000 lb	40 knots tow speed
R	= 930 ft	40 knots tow speed

[9] Calkins, D.E., "Hydrofoil High-Speed Towed System: Trial Evaluation, Part III," NUC TP 241 (Aug 1972).

$$\xi_\alpha - \xi_T \quad = 0.269 \text{ inch}$$

Inserting these values into equation (41) yields,

$$\xi_\alpha - \xi_T \geq 0.0000724 \text{ inch}$$

which is obviously satisfied.

EFFECT OF TORSIONAL RIGIDITY

The effect of torsional rigidity, $\overline{GJ}$, can be determined by solving the complete twist equation (21). Substituting the $\hat{M}$ components from equation (17) and m_s from equation (15) yields

$$\overline{GJ}\,\frac{d\tau}{ds} + (\overline{EI}_2 - \overline{EI}_1)(\alpha K_n^{\,2} - \alpha K_k^{\,2} - K_n K_k) + T(\xi_T - \xi_s)(K_k - \alpha K_n) + m(\alpha)\sin^2\phi = 0 \tag{42}$$

Closed form solutions to equation (42) for general functions T(s) and $\phi(s)$ are not possible. A simpler but useful problem can be formulated by assuming that the basic trail catenary is nearly vertical and with a radius of curvature large compared to total scope, L. Thus if $dL/T_o = \delta$ is considered a small parameter, then the following approximations are valid:

$$\begin{aligned} T/T_o &= 1 + 0(\delta^2) \\ L \cdot K_n &= \frac{d\phi}{d\mathcal{s}} = -\delta + 0(\delta^2) \\ L \cdot K_k &= -\delta(\ell/d) + 0(\delta^2) \\ L \cdot \tau &= \frac{-d\alpha}{d\mathcal{s}} - \delta^2 \mathcal{s}\,\frac{\ell}{d} + 0(\delta^3) \end{aligned} \tag{43}$$

where $\mathcal{s} = s/L$. Inserting these expressions into equation (42) regarding $\ell/d \sim 0(1)$ and retaining terms of order α and δ^2 gives

$$\frac{d\alpha}{d\mathcal{s}} - \frac{d\alpha}{d\mathcal{s}} + \delta^2 \mathcal{s}\,\frac{\ell(\alpha)}{d} + \left(\frac{\frac{T_o^{\,2}}{d}(\xi_T - \xi_s) + \overline{EI}_2 - \overline{EI}_1}{\overline{GJ}}\right)\delta^2\,\frac{\ell(\alpha)}{d} + \frac{m(\alpha)}{\overline{GJ}}\,L^2 = 0 \tag{44}$$

If the approximation of equation (40) is used for $m(\alpha)$ and equation (12) for $\ell(\alpha)$, then in terms of the variable s^*,

$$s^* = \mathcal{s}\,\delta\sqrt{\frac{\left(\frac{dC_\ell}{d\alpha}\right)}{C_d}}_{\alpha = 0} \tag{45}$$

one obtains, after some manipulation,

$$\frac{d^2\alpha}{ds*^2} + s* \frac{d\alpha}{ds*} + Q\,\alpha = 0 \qquad (46)$$

where the constant Q is given by

$$Q = \frac{\overline{EI}_1 - \overline{EI}_2 + \overline{GJ} - \frac{To^2}{d}(\xi_\alpha - \xi_T)}{\overline{GJ}} \qquad (47)$$

The general solution of equation (46) may be written as

$$\alpha(s*;\,Q) = e^{-\frac{1}{2}s*^2}\left\{C_1\, m\,(\tfrac{1}{2} - \tfrac{Q}{2}, \tfrac{1}{2}, \tfrac{1}{2}\, s*^2) + C_2\, s*\, m\,(1 - \tfrac{Q}{2}, \tfrac{3}{2}, \tfrac{1}{2}\, s*^2)\right\} \qquad (48)$$

where $m(a,b,x,)$ is the confluent hypergeometric function. If the fairing is free swivelling at its terminations, $[\tau(o) = \tau(L) = 0]$ then nontrivial solutions are possible only if

$$m\,(\frac{3}{2} - \frac{Q}{2}, \frac{3}{2}, \frac{1}{2}\, s_L^{*2}) = 0 \qquad (49)$$

where $s_L^* = s*$ at $s = L$. The smallest value of s_L^* for which equation (49) is satisfied may be found by using Abramowitz[10] formula for x_o, the first positive zero of $m\,(a,b,x)$,

$$x_o \approx \frac{\pi^2 (\frac{1}{4} + \frac{b}{2})^2}{2b - 4a}$$

Applying this to Equation (49) yields the stability requirement

$$\frac{1}{2}\, s*^2 \le \frac{\pi^2}{-3 + 2Q} \qquad (50)$$

or, equivalently,

$$\xi_\alpha - \xi_T \ge -\frac{\pi^2\,\overline{GJ}}{\left(\frac{d\ell}{d\alpha}\right)L^2} + \frac{\overline{EI}_1 - \overline{EI}_2 - \frac{1}{2}\overline{GJ}}{T_o\, R_o} \qquad (51)$$

where $R_o = T_o/d$ is the radius of curvature.

[10] Abramowitz, M. and I. Stegun, "Handbook of Mathematical Functions," Chapter 13, U.S. Government Printing Office, Washington, D.C., 1965

If the cable is free swivelling at $s = L$ ($\tau(L) = 0$), but built in at $s = 0$ $(\vec{e}_z \cdot \vec{e}_2 = 0)_{s=0}$, then in a similar manner one obtains the relation of equation (51) except for a factor of 1/4 on the first term of the right-hand side. These results may be compared to the extreme case of a vertical cable ($dL/T_o \rightarrow 0$) for which the twist equation reduces to

$$\frac{d^2\alpha}{ds^2} - \lambda\,\alpha = 0; \quad \lambda = \frac{\left(\frac{d\ell}{d\alpha}\right)_{\alpha=0} \quad (\xi_\alpha - \xi_T)}{\overline{GJ}} \tag{52}$$

If $\lambda > 0$, stable solutions are assured. If $\lambda < 0$, then the general solution is

$$\alpha = C_1 \sin\sqrt{-\lambda}\, s + C_2 \cos\sqrt{-\lambda}\, s \tag{53}$$

and for which stability is assured if

$$\begin{aligned} -\lambda &< \frac{\pi^2}{L^2} \quad \frac{d\alpha}{ds} = 0 \quad \text{at } s = 0,\ L \\ -\lambda &< \frac{1}{4}\,\frac{\pi^2}{L^2} \quad \frac{d\alpha}{ds} = 0 \quad s = L \\ & \qquad\qquad \alpha = 0 \quad s = 0 \end{aligned} \tag{54}$$

These are equivalent to the solution given by equation (51) for $\frac{dL}{To} \rightarrow 0$. Thus, the effect of $\overline{GJ}$ is seen to be stabilizing in two ways. First, there is an end effect (usually very small for realistic fairing lengths) dependent on the type of end fixity. Second, there is a stabilizing term associated with the curvature in the same manner as the flexural rigidities.

It is interesting to note that in the case of a straight line catenary, if $\lambda > 0$, the solution with $\alpha(0) = \alpha_o$ and $d\alpha/ds = 0$ at $S = L$ is

$$\alpha = \alpha_o \frac{\cosh\sqrt{\lambda}\,(L-s)}{\cosh\sqrt{\lambda}\,L}$$

and as $\sqrt{\lambda}\,L \rightarrow \infty$, $\frac{\alpha}{\alpha_o} \rightarrow e^{-\sqrt{\lambda}\,s}$. Thus, the effect of towed body torque (or, for that matter, a torsional disturbance anywhere along the fairing) exponentially decays from the point of application.

CONCLUSIONS

A theory for the hydrodynamic and structural mechanisms leading to faired towline kiting is presented. Stability criteria and relationships for predicting towing performance are developed in terms of the fairing section geometric properties, structural characteristics, and hydrodynamic coefficients. Specifically, it is found that:

1) A small angle of attack, constant along the faired towline is sufficient to cause catastrophic kiting. For a lift/drag ratio of unity ($\alpha \approx 0.15$ degree), kite angles up to 60 degrees can result (Figure 5), with a corresponding depth loss of 10 to 15 percent (Figure 7) and body lateral displacement of 40 percent of scope (Figure 6).

2) Remarkably small fairing section asymmetries (0.1 percent of chord), if constant spanwise, result in sufficient angle of attack for severe kiting. The degree of this camber induced kiting is critically dependent on the chordwise locations of hydrodynamic and tension loading.

3) Flexural rigidity, in combination with the towing catenary curvature can result in a destabilizing twist moment. A criteria for the required hydrodynamic moment arm to overcome this effect is given in equation (41).

4) Torsional rigidity acts to stabilize the fairing in twist, depending on end constraints and catenary curvature as shown in equation (51).

The foregoing analysis will provide criteria for designing improved faired towline strength members and fairings while minimizing the risk of kiting. The theory also provides a general framework which could be extended to investigate, for example, dynamic stability.

ACKNOWLEDGMENTS

The author would like to thank Messrs. D. Dillon, S. Gay and Dr. H. Wang for their helpful discussions in the course of this work.

REFERENCES

1. Abkowitz, M.A., "The Stability of a Faired Cable of a Tethered System in its Fundamental Mode," Joseph Kaye and Co., Inc., Report 73, Sept 1967.
2. Hegemeir, G.A., "Divergence Criteria for a Faired Towcable in a Sub-cavitating Flow," University of California, San Diego, June 1968.
3. Dillon, D.B., "The Configuration and Loading of a Torsionally Elastic Faired Cable," Hydrospace-Challenger, Inc., TR-4557-001, Oct 1973.
4. Wang, H.T., "A FORTRAN IV Program for the Three-Dimensional Steady-State Configuration of Extensible Flexible Cable Systems," Naval Ship Research and Development Center, Research and Development Report 4384 (Sept 1974).
5. Hildebrand, F., "Advanced Calculus for Applications," Chapter 6, Prentice-Hall, Inc., New Jersey, 1962.
6. Casarella, M.J. and M. Parsons, "Cable Systems Under Hydrodynamic Loading," M.T.S. Journal, Vol. 4, no. 4, July - August 1970.
7. Folb, R., "Experimental Determination of Hydrodynamic Loading for Ten Cable Fairing Models," SPD R&D Report 4610 (in progress)
8. Love, A.E.H., "A Treatise on the Mathematical Theory of Elasticity," Chapter 18, Dover, New York, 1944.
9. Calkins, D.E., "Hydrofoil High-Speed Towed System: Trial Evaluation," Part III, NUC TP 241, August 1972.
10. Abramowitz, M. and Stegun, I., "Handbook of Mathematical Functions," Chapter 13, U.S. Government Printing Office, Washington, D.C., 1965.

PRECEDING PAGE BLANK-NOT FILMED

INITIAL DISTRIBUTION

Copies

1 CNO, Attn: OP098T6
  Mr. H. Cheng

4 NAVMAT
  1 MAT 0331
  3 MAT 03422

2 NRL
  1 Code 2027
  1 Dr. James McGrath

2 NAVAIRDEVCEN
  Johnsville, Warminster, Pa. 18974
  1 Tech Lib
  1 Code 2063

2 NAVAIRSYSCOM
  1 AIR 5330
  1 AIR 370

6 NAVSEASYSCOM
  1 SEA 037
  1 SEA 00
  1 SEA 09G32 (SHIPS 2052)
  1 SEA 033 (ORD 035)
  1 PMS 393
  1 PMS 395

1 Commander, Naval Facilities Engr Comm

1 Naval Underwater Systems Center
  New London, Conn. 06320
  Attn: Lib

2 CO&DIR, Naval Civil Engr Lab
  Port Hueneme, Calif. 93401
  1 Code L31, Lib
  1 Code L44, F.C. Liu

1 U.S. Naval Academy, Lib

1 U.S. Naval Postgraduate School, Lib

12 DDC

Copies

1 Library of Congress
  Sci & Technology Div

1 U.S. Coast Guard, Attn: Division of Merchant Marine Safety

1 NOAA Data Buoy Center

1 NASA Scientific & Technical Information Facility

1 National Science Foundation,
  Engr Div
  Attn: Director

1 CHONR
  Attn: Mr. Ralph D. Cooper
  Code 438

1 Univ of California
  Scripps Inst. of Oceanography
  Attn: Mr. J. Pollack

1 Catholic Univ
  Inst. of Ocean Science & Engr
  Attn: Prof. M.J. Casarella

1 Harvard Univ, Pierce Hall
  Attn: Prof. G.F. Carrier

3 MIT, Dept of NAME
  1 Department Chairman
  1 Prof. Abkowitz
  1 Prof. Kerwin

1 U.S. Merchant Marine Academy
  Attn: Capt. L.S. McCready

2 Oregon State Univ
  Civil Engr Dept
  1 Dr. J.H. Nath
  1 Dr. S. Neshyba

2 Univ of Pennsylvania
  The Towne School of Civil & Mechanical Engr
  1 Prof. B. Paul
  1 Prof. A. Soler

Copies

1 Purdue Univ
Dept of Aeronautical Engr
Attn: Prof. J. Genin

1 Rutgers Univ, Dept of Mechanical & Aerospace Engr
Attn: Prof. S.P. Reyle

2 Stevens Inst of Technology
Davidson Laboratory
Attn: Lib
1 Dr. J.P. Breslin

2 SWRI
1 Dr. H. Abramson
1 Applied Mechanics Review

2 Texas A&M, Dept of Oceanography
1 Prof. R.O. Reid
1 Prof. B.W. Wilson

1 Univ of Washington
Applied Physics Lab
Attn: Director

1 Woods Hole Oceanographic Inst
Attn: Ocean Engr Dept

1 Hydronautics, Inc.
Mr. M. Altman

1 Hydrospace-Challenger, Inc.
Mr. D.B. Dillon

1 Mar, Inc.

1 Oceanics, Inc.
Dr. Paul Kaplan

1 Ocean Science & Eng, Inc.
Mr. Robert Snyder

1 SNAME

1 Tracor, Inc.

1 Westinghouse Ocean Science & Engineering Facility

Copies

3 Webb Inst of Naval Architecture
Crescent Beach Road
Glen Cove, L.I., N.Y. 11542
Attn: Prof. E.V. Lewis (1)
Prof. L.W. Ward (1)
Prof. D. Hoffman (1)

1 California Institute of Technology
Pasadena, California 91109
Attn: Prof. T.Y. Wu

CENTER DISTRIBUTION

Copies	Code
1	15
1	152
1	154
25	1544, B. Cox
5	1548, R. Folb
3	1552 1 J.H. McCarthy 1 H.T. Wang 1 K.P. Kerney
1	156
1	1576
30	5211 Reports Distribution
1	5221 Main Library
1	5222 Annapolis Library

END

DATE
FILMED

3-76